Biomedicine & Pharmacotherapy 200 (2026) 119546

Contents lists available at ScienceDirect

Biomedicine & Pharmacotherapy

journal homepage: www.elsevier.com/locate/biopha

Late-stage modification of the alkaloid toxin veratridine to photocontrol excitable tissues

Luisa Camerin [a,b,c], Galyna Maleeva [a,b], Ailín Ramírez-Abreu [a,b,d], Víctor Cilleros-Mañé [a,b], Drilon Miftari [e,f], Montserrat Batlle [e,f], Carlo Matera [a,b,g], Eduard Guasch [e,f], Pau Gorostiza [a,b,h,*]

[a] Institute for Bioengineering of Catalonia (IBEC), The Barcelona Institute for Science and Technology (BIST), Spain
[b] Networking Biomedical Center in Bioengineering, Biomaterials, and Nanomedicine (CIBER-BBN), ISCIII, Spain
[c] Doctorate program in Organic Chemistry, University of Barcelona, Spain
[d] Doctorate program in Drug Research, Development and Control, University of Barcelona, Spain
[e] Institut Clínic Cardiovascular, Hospital Clinic, University of Barcelona (UB), IDIBAPS, Barcelona, Spain
[f] Networking Biomedical Center in Cardiovascular Diseases (CIBER-CV), ISCIII, Spain
[g] Department of Pharmaceutical Sciences, University of Milan, Milan, Italy
[h] Catalan Institution for Research and Advanced Studies (ICREA), Spain

ARTICLE INFO

Keywords:
Natural product
Veratridine
VTD
Steroid
Veratrum
Voltage-gated sodium channel (VGSC)
Inactivation
Opener
Agonist
Antihypertensive
Azobenzene
Photochromism
Photoswitch
Photoswitchable toxin
Neuromodulation
Cancer
Photopharmacology
Optopharmacology

ABSTRACT

Natural products and their structural derivatives have long played a crucial role in the discovery of new medical treatments and pharmacotherapies. However, certain natural compounds, such as toxins, are classified as hazardous substances that pose risk to human health. It is desirable to modulate the activity of toxins to minimize their harmful effects and unleash their potential as selective and bioavailable drugs. Yet, the functionalization of natural products remains a challenge due to their structural complexity. Here, we present two methods for late-stage C-H nitration and subsequent derivatization of the alkaloid steroidal neurotoxin veratridine, a sodium channel opener, by introducing an azobenzene photoswitch in its structure. The resulting compound, Azoveratridine, displays aqueous solubility, reversible photoisomerization, and light-dependent activity in neurons and myocardial slices.

1. Introduction

For more than a century, pharmacology has struggled to devise synthetic compounds with high potency, efficacy, and bioavailability to target a diversity of proteins in our bodies. High-throughput synthesis, screening, iterative optimization, and more recently computer-aided design are deployed to discover drug candidates that often end up showing limited clinical efficacy [1].

Nature had millions of years of head start to evolve powerful organic compounds and peptides that activate or block essential proteins for survival like ion channels and receptors [2], and that are used for the purpose of defense [3,4], predation [5], and symbiosis [6,7]. They are present in all taxa from bacteria to fungi, plants, and animals, and exploit highly conserved molecular structures underlying key protein functions [8].

Toxins are organic molecules with intricate structure and complex

* Corresponding author at: Institute for Bioengineering of Catalonia (IBEC), The Barcelona Institute for Science and Technology (BIST), Spain.
E-mail address: pau@icrea.cat (P. Gorostiza).

https://doi.org/10.1016/j.biopha.2026.119546
Received 19 February 2026; Received in revised form 15 May 2026; Accepted 18 May 2026
Available online 25 May 2026

biosynthetic pathways [9] which have been fully appreciated only when humans have achieved to replicate them by total synthesis [10–13]. They possess extremely high pharmacological potency, efficacy, and wicked kinetics and biodistribution. Conotoxins from marine snails kill their preys in seconds by inhibiting their nicotinic acetylcholine receptors and voltage-gated sodium, potassium, and calcium ion channels [14]. The lethal dose of tetrodotoxin (TTX, a sodium channel blocker) is 8 μg/kg [15], that of maitotoxin (an activator of calcium channels) is 0.1 μg/kg [16], and that of tetanus and botulinum toxins are a few ng/kg in mice [17]. Venoms contain highly potent and fast-acting toxins that display lower bioavailability and must be injected with specially evolved stings or fangs.

Toxins entail fascinating chemistry and a broad variety of medical applications to treat pain, hypertension, strabismus, muscle dystonia, hyperhidrosis, urinary incontinence, and migraine [18,19]. However, the power of toxins must be harnessed to avoid adverse effects. The activity of peptide and protein toxins can be altered by chemical and genetic modification of their amino acids [20–25], while traditional functionalization strategies for small molecule natural products typically rely on early-stage derivatization or total synthesis, both of which are time- and resource-intensive. Moreover, late-stage functionalization methods are limited, and they have never been used to remotely control the activity of natural toxins. Here, we developed a conjugation strategy for late-stage modification of a natural toxin, the homosteroidal alkaloid veratridine (Fig. 1) from the poisonous plant *Veratrum album*. We have validated this late-stage derivatization approach by introducing a photoisomerizable azobenzene group that enables to control with light the activity of veratridine in neurons and in cardiac tissue.

The resulting compound, Azoveratridine (Fig. 1), can be activated by ultraviolet light, it switches back reversibly with blue light, and it retains the micromolar potency and aqueous solubility of the parent compound [26]. Our synthetic route —starting with the nitration of the original toxin in mild conditions— may accommodate the introduction of diverse groups including azobenzenes with tuned photochemical properties, fluorescent and radioactive labels, and reactive moieties for further selective functionalization.

By harnessing the power of toxins with light, we contribute a novel class of photoswitchable drugs to the photopharmacological toolbox and enable new opportunities for fundamental research and for reducing adverse effects in therapeutic applications.

2. Results and discussion

2.1. Design and synthesis of Azoveratridine

Several toxins target voltage-gated sodium (Na_V) channels, which are important in neuronal and muscular signaling. Veratridine can act as a partial agonist of Na_V channels by first inducing channel opening and then inhibiting inactivation, allowing a continuous influx of sodium ions into the cell [27,28]. Although the exact binding pocket and key interactions of veratridine in Na_v channels have not been experimentally determined, this toxin has been suggested to bind inside the ion pore in cardiac $Na_V1.5$ channels and near the cytoplasmic mouth of skeletal muscle $Na_V1.4$ channels [28–30]. Based on these reports [28,30], we performed molecular docking simulations to qualitatively explore potential binding modes of veratridine and its photoswitchable derivative, Azoveratridine, in both *cis* and *trans* isoforms, at both proposed binding sites. The simulation results indicate that neither veratridine nor Azoveratridine bind at the extracellular mouth of the pore in $Na_V1.4$ (PDB: 6AGF). In contrast, the inner pore of $Na_V1.5$ (PDB: 6LQA) accommodates both the toxin and its photoswitchable derivative (see Supporting Information section 1.4 for details).

To introduce a photoswitchable group in the toxin without altering its binding properties, we examined the possibilities for selective modification. The chemical structure of veratridine is complex and rich in chiral centers and reactive functional groups. The latter include glycosidic bonds, free hydroxyl, ester, and a benzene ring that offers the possibility of introducing an azobenzene by azo-extension [31] to yield Azoveratridine (**1**, Fig. 1). Considering the risk of toxicity, high potency, and cost of veratridine, we initially explored regioselective synthetic accessibility with the commercially available model compound methyl 3,4-dimethoxybenzoate, which mimics the toxin aromatic tail (**2**, Fig. 1). However, the essential role of the veratroyl ester moiety for veratridine activity [28,30,32,33] prompts verifying that the full toxin retains activity after modification.

Since one-step derivatization for natural products is desirable for higher yields, cost- and time-effectiveness, and reduced waste, we first attempted the introduction of the azobenzene on the veratroyl moiety by azo coupling via diazonium salt formation. The synthetic efforts are summarized in Scheme S1 (SI) by the attempts to couple diazonium salts starting from three different commercially available reagents (aniline, 4-methoxybenzenediazonium tetrafluoroborate and 2-fluoro-4-nitroaniline), all of which failed. Aniline was readily converted to the diazonium salt intermediate **3**, but instead of reacting with reagent **2** as intended, it preferentially underwent coupling with residual aniline, forming an undesired side product. This outcome persisted under various conditions (see SI Scheme S1.A; Figure S1, and Table S1 for details). To overcome the formation of the side product, we used the commercially available diazonium salt 4-methoxybenzenediazonium tetrafluoroborate as an alternative starting material (SI Scheme S1.B). However, this approach also failed to produce the desired azo compound. The lack of reactivity may be attributed to the methoxy group in the *para* position, whose electron-donating nature likely reduces the electrophilicity of the diazonium centre. Seeking a more reactive system,

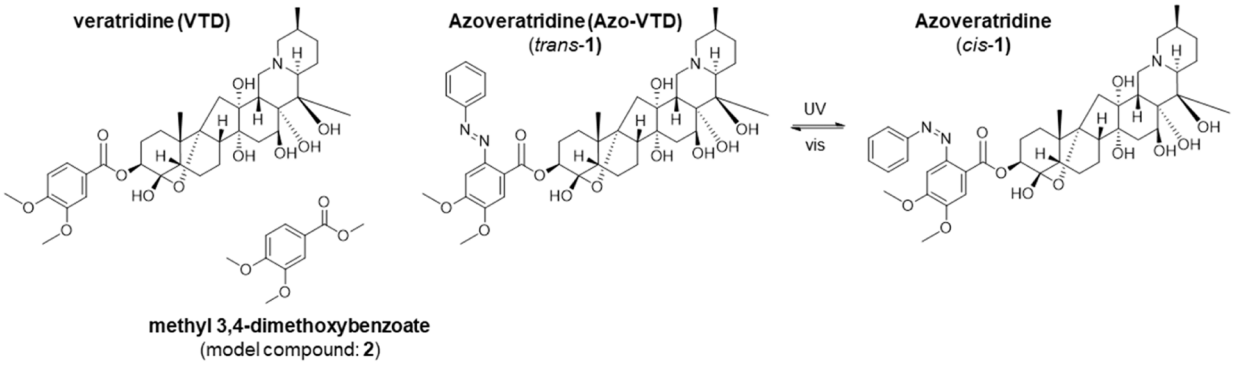

Fig. 1. Design of a photoswitchable analog of veratridine by late-stage modification. Structure of veratridine (VTD), a homosteroidal alkaloid toxin, and design of its azobenzene-substituted analog, Azoveratridine (Azo-VTD, 1), which can photoisomerize between the *cis* and *trans* conformations respectively using UV and visible light. Methyl 3,4-dimethoxybenzoate (2) is a model compound of the toxin aromatic tail (veratroyl ester) that we used to explore synthetic modification strategies prior to their application on veratridine.

we then employed 2-fluoro-4-nitroaniline, featuring electron-withdrawing groups expected to enhance diazonium electrophilicity (SI Scheme S1.C). Even so, no reaction was observed under the tested conditions.

Since single-step azo coupling via diazonium salt proved unsuccessful, we followed an alternative synthetic route to introduce the azobenzene through a Baeyer-Mills reaction. To achieve this, it was essential to establish suitable conditions for the late-stage functionalization of veratridine by introducing a nitro group without causing degradation or impacting other functional groups within the toxin. Classical nitration reactions, which typically involve harsh acidic conditions with sulfuric and nitric acid, risked compromising the toxin's complex structure by breaking esters and/or glycoside bonds. Consequently, we explored milder nitration conditions and initially tested the reactions on methyl 3,4-dimethoxybenzoate (**2**) as reported in Scheme 1.

We began by using a metal catalyst and a stoichiometric amount of nitric acid. Several combinations of solvents and two different metal catalysts were tested to improve the nitration yield as reported in SI Table S2. The highest yield (66%) to afford compound **8** (Scheme 1) was achieved in toluene with penta-ammine-chloridocobalt (III) dichloride ($[Co(NH_3)_5Cl]Cl_2$) as catalyst. The Co(III)/HNO_3 nitration displayed a pronounced solvent effect (Table S2): productive conditions were found only in non-coordinating solvents (toluene > DCM ≈ $CHCl_3$), while coordinating oxygenated/protic solvents (THF, dioxane, DMF, MeOH, EtOH) completely suppressed conversion. This trend suggests that solvent coordination or trapping of the active nitrating species, as well as differences in solubility/availability of the cobalt complex, may dominate over simple correlations with boiling point or bulk polarity. Once the nitro group was successfully introduced, catalytic hydrogenation in the presence of palladium on carbon afforded the corresponding amine **9** (quantitative conversion) which was used without further purification. The amine was subsequently coupled with nitrosobenzene under classical Baeyer-Mills conditions affording the desired product **4** in 52% yield. Since the synthetic route was successful with the model compound **2**, we decided to apply it to veratridine. However, the initial nitration step caused the full degradation of veratridine, even in the presence of stoichiometric amount of nitric acid.

Therefore, two additional reaction conditions were investigated for the nitration step. The nitration of the model compound **2** was also achieved with potassium nitrate (KNO_3) in presence of trimethylsilyl chloride (TMSCl) and subsequent addition at 0 °C of aluminium chloride ($AlCl_3$). Encouraged by the positive outcome, we tested the same conditions on veratridine and monitored the progression of the reaction by liquid chromatography–mass spectrometry (LCMS). These conditions enabled the nitration of veratridine, although several additions of the commercial reagents (KNO_3, TMSCl and $ALCl_3$) were necessary until the reaction did not proceed any further. However, repeated attempts at functionalizing veratridine showed inconsistencies, with cleaner reactions and fewer impurities achieved only on a smaller scale (see SI Table S3 and SI Scheme S3 for details on veratridine reactions).

To improve the yield, reduce the formation of impurities, and enhance the reproducibility, we also performed the reaction using nitronium tetrafluoroborate (BNO_2F_4) as nitrating agent. We tested these conditions first on reagent **2** using dry organic solvents in an inert atmosphere of nitrogen to prevent the degradation of BNO_2F_4 (see SI Table S4 for reactions details). Initially, reagent **2** was dissolved in dry dichloromethane (DCM) and BNO_2F_4 was added in sulfolane solution 0.5 M. However, the extraction with water failed to remove sulfolane from the reaction crude. Powdered BNO_2F_4 was more effective and enabled an easier work-up, achieving 65% yield. Since the nitration with BNO_2F_4 proceeded smoothly with the model compound **2**, we tested it on veratridine and monitored the reaction by LCMS (see Scheme 2). After 24 h of stirring, we observed the formation of nitrated veratridine **10** together with unreacted starting material. A second addition of BNO_2F_4 and stirring for another 8 h led to reaction completion, whereas stirring for longer increased the impurities. We repeated this reaction three times on veratridine, confirming the reproducibility of these conditions. Since the nitrated veratridine **10** was partially soluble in water, extraction was avoided, and the crude was directly purified by chromatography to isolate pure product **10**. Reduction of the nitro group through hydrogenation in the presence of palladium on carbon yielded the corresponding amine compound **11** in good yield (70%). Finally, we obtained the azo-derivatized veratridine **1** via azo coupling with nitrosobenzene in acetic acid. This reaction, carried out over 5 days with multiple additions of nitrosobenzene, achieved a moderately good yield of 22%.

2.2. Photochemical characterization of Azoveratridine

We assessed the photochemical behavior of Azoveratridine (**1**) in 0.1 M phosphate buffered saline (PBS) solution using a UV–vis spectrophotometer. The compound absorbance in the dark-relaxed form (benchtop condition) is reduced by isomerization to the *cis* isoform under 365 nm light and can be increased again using 475 nm light (Fig. 2.A). Azoveratridine can be reversibly and repeatedly photoswitched with UV and visible light without any loss of absorbance that may indicate degradation and thus shows resistance to photofatigue (Fig. 2.B). The photostationary state (PSS) was quantified using high-performance liquid chromatography (HPLC) by analysing chromatograms from the diode array at the isosbestic wavelength (257 nm), where the molar absorption coefficients of both isomers are equivalent. HPLC chromatograms in Fig. 2.C show partial photoconversion (67% *cis* under 365 nm light and 56% *trans* under 475 nm light) and detect the presence of 26% *cis* isomer in the dark-relaxed form at the benchtop condition. Heating the benchtop solution at 50 °C for 96 h reduces the *cis* fraction to 3% but at the cost of partial degradation (see SI Figures S12 and S13). We also studied the spontaneous thermal relaxation of UV-irradiated Azoveratridine in dark conditions at room temperature. Over the recorded time frame of 13 h, the compound did not show significant recovery in absorbance at λ = 350 nm, indicating that the thermal relaxation process is slow under these conditions and the *cis* form is particularly stable (SI Figure S8.C). Overall, Azoveratridine shows robust photochemical properties in agreement with typical

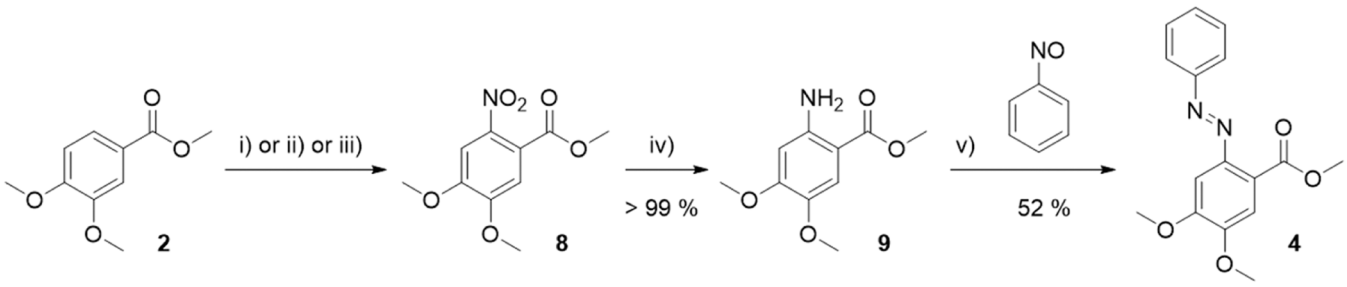

Scheme 1. Reaction conditions: i) $[Co(NH_3)_5Cl]Cl_2$, HNO_3 69%, toluene, 5 days, rt, 66% yield; or ii) TMSCl, KNO_3 and $AlCl_3$, DCM, 83% yield; or ii) BNO_2F_4, dry DCM, 0°C to rt, 65% yield. iv) Pd/c, 1 atm H_2, EtOH, 72 h, rt. v) AcOH, nitrosobenzene, rt.

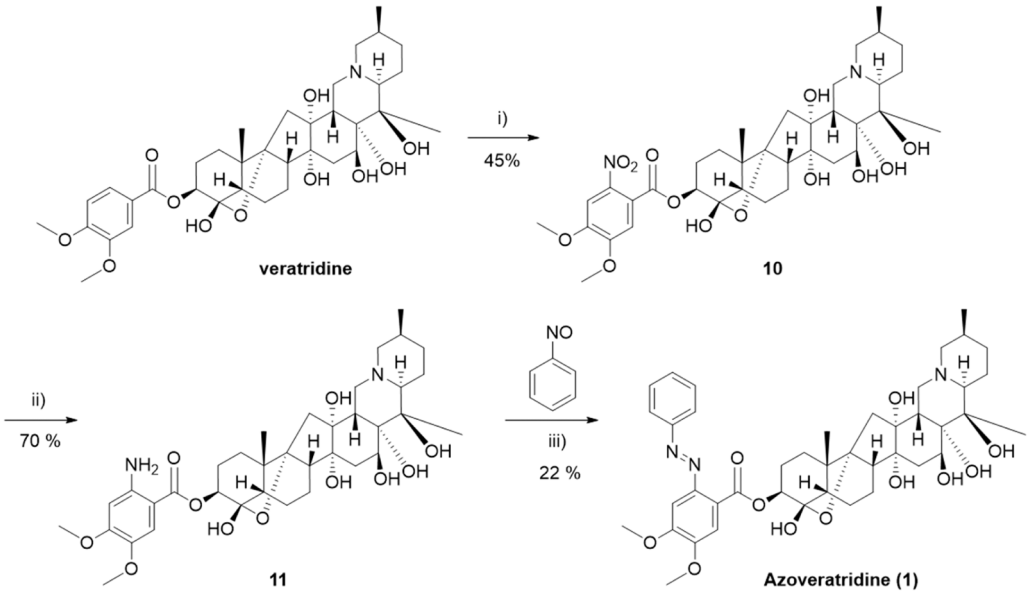

Scheme 2. Reaction conditions: i) BNO_2F_4, dry DCM, 0°C to rt. ii) Pd/C, 1 atm H_2, EtOH. iii) Nitrosobenzene, AcOH, under N_2.

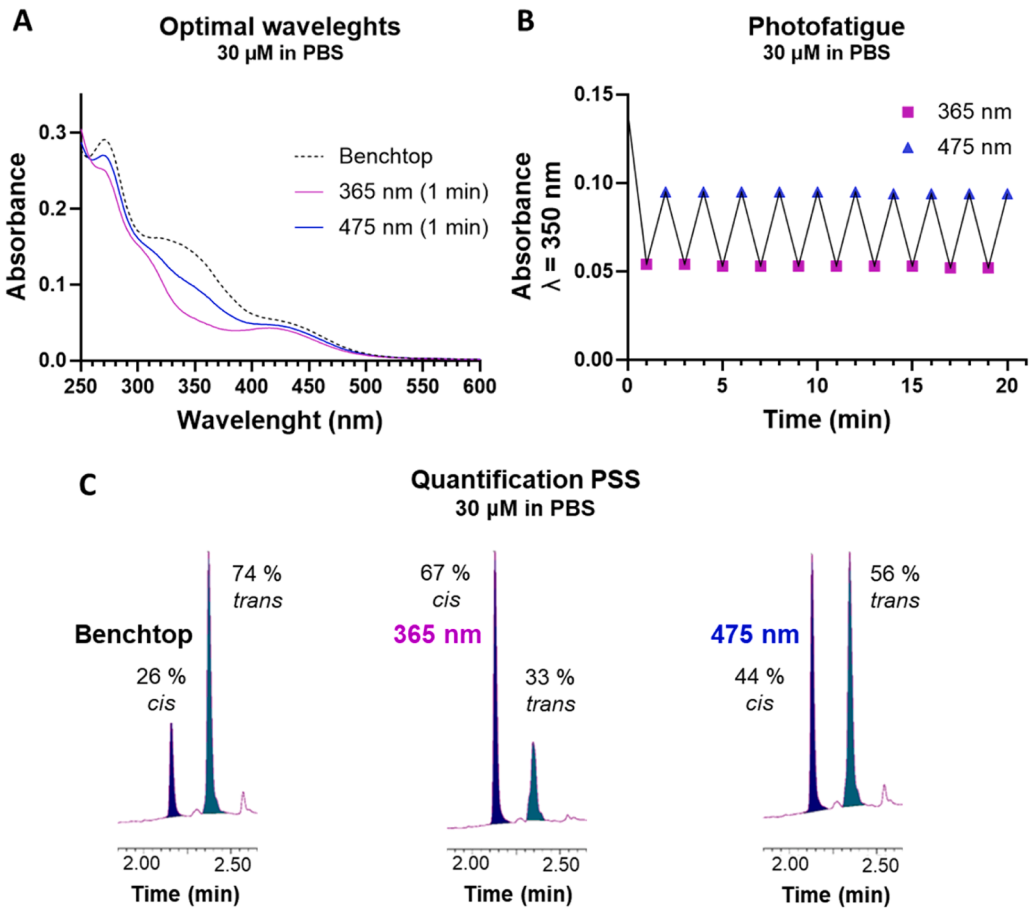

Fig. 2. Photochemical properties of Azoveratridine (1). A) Azoveratridine can be isomerized from *trans* to *cis* under 365 nm irradiation and from *cis* to *trans* under 475 nm irradiation. B) Reversible photoisomerization and resistance to photofatigue are observed upon several cycles of illumination without loss in absorbance. C) HPLC chromatograms allow to quantify the photostationary states (PSS) at benchtop conditions before irradiation (74% *trans*, 26% *cis*), after irradiation at 365 nm for 1 min (33% *trans*, 67% *cis*) and after 475 nm irradiation for 1 min (56% *trans*, 44% *cis*). All photochemical experiments including the evaluation of thermal back-isomerization were carried out in PBS 0.1 M at 25 °C.

azobenzene features, allowing to test the activity of *trans*- and *cis*-enriched solutions.

To complement these results, compound **4** was also photochemically characterized and it exhibited similar properties with optimal

isomerization wavelengths of 365 nm and 475 nm (Figure S9). In addition, no thermal relaxation was observed at room temperature over the recorded time frame of 800 min, suggesting that the presence of the steroidal group in the toxin does not influence the thermal relaxation behaviour. Instead, thermal relaxation likely depends on the substitution pattern of the azobenzene moiety. Indeed, it has been reported that different substituents, the presence of hetero atoms—or the same substituent positioned differently on the aromatic rings—can significantly affect the kinetics of thermal relaxation [34–39].

Finally, we studied heat-induced thermal relaxation by exposing the solutions of Azoveratridine (30 μM in PBS) and compound **4** (50 μM in PBS) at 50 °C in order to induce the maximum *trans* conversion. For Azoveratridine, the starting point was the benchtop solution containing 74% *trans* isomer, while for compound **4** we used the solution obtained after 475 nm irradiation, containing 66% *trans* (Figure S12 and Figure S14). Despite partial degradation due to heat (Figure S13), Azoveratridine reached a maximum conversion of 97% *trans* after 96 h 50 °C, corresponding to a half-life ($t_{1/2}$) of 30 h under these conditions (Figure S15.A). Compound **4** reached a maximum conversion of 91% *trans* (the same as its benchtop condition) after 72 h, with a $t_{1/2} = 20$ h (Figure S15.B).

2.3. Azoveratridine photocontrols neural and cardiac activity

To evaluate the biological activity of Azoveratridine, we examined the effects of *cis*- and *trans*-enriched solutions on excitable cells, including hippocampal neurons and myocardial slices, which express Na_V channels and are known to be influenced by veratridine binding [28,40]. Na_V channels drive action potentials in neurons by opening their Na^+ -permeable pore in response to membrane depolarization beyond a specific threshold. Pore opening allows an influx of Na^+ ions that further depolarizes the membrane and propagates the activation

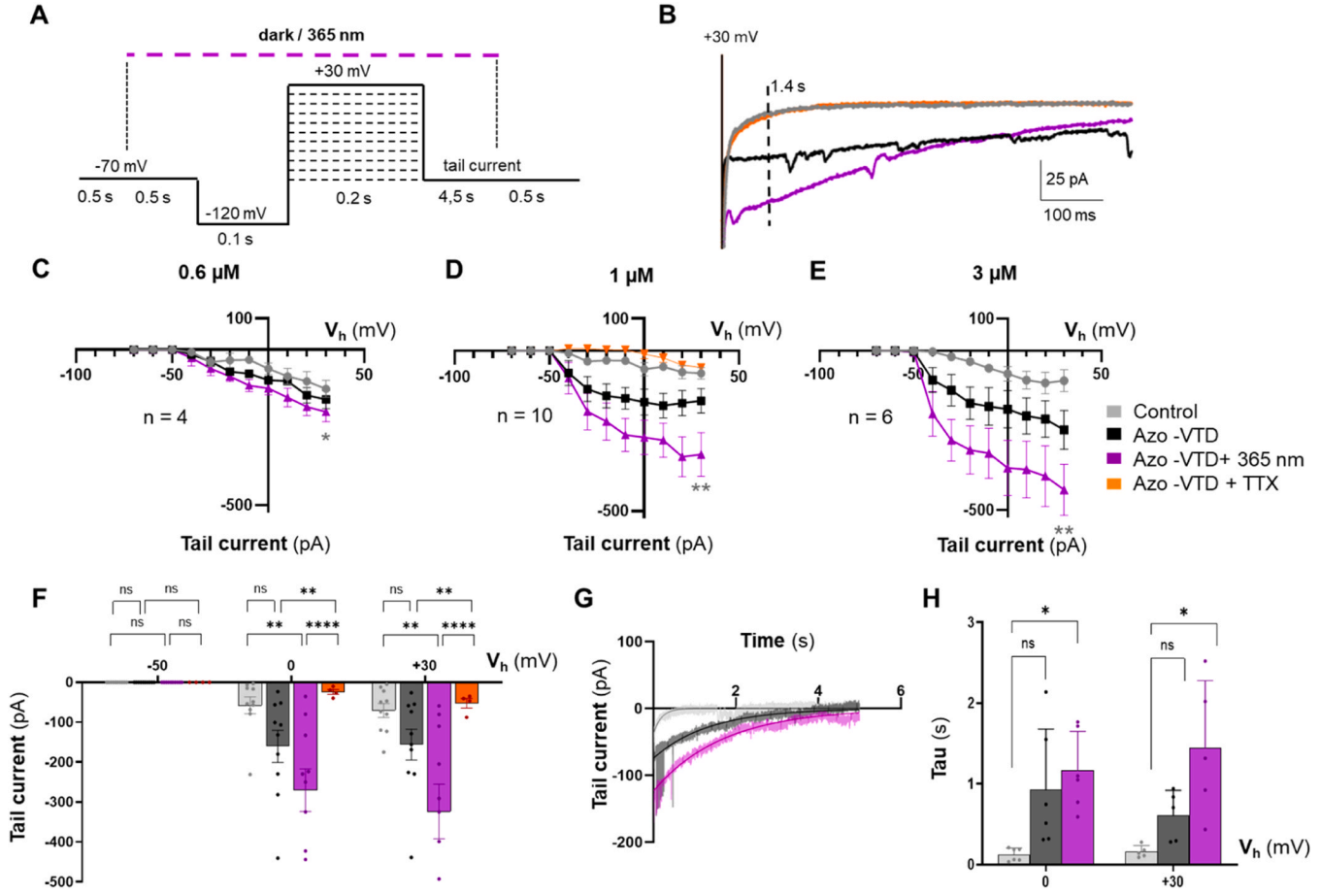

Fig. 3. Effect of Azoveratridine (Azo-VTD) and UV illumination on voltage-gated Na^+ currents of cultured primary hippocampal neurons. A) Scheme of the membrane potential pulse protocol applied with patch-clamp to generate Na^+ currents and duration of 365 nm light application. B) Tail current traces in the absence of Azoveratridine (control, i.e., zero-current baseline, plotted in gray), with 1 μM Azoveratridine in the dark (black plot), during 365 nm illumination (violet plot) and after addition of 1 μM tetrodotoxin (TTX) to block Na_V currents (plotted in orange and nearly overlapping with the control curve). All recordings were done at V_{hold} = +30 mV. The dashed vertical line indicates the time point at which current amplitude was quantified (1.4 s). Small deflections on the black and violet traces correspond to the synaptic currents that were regularly present in some recording due to the composition of intracellular solution that was used. C, D, E,) Current-voltage plots of the tail current amplitude measured at 1.4 s in the absence of Azoveratridine (gray), with 0.6 μM (C), 1 μM (D), and 3 μM (E) of Azoveratridine (black), and during illumination with 365 nm (violet). Addition of 1 μM TTX (orange) abolishes the effect of *cis*-Azoveratridine (panel D). Each data point represents the mean ± SEM from 4 to 10 independent cells. Statistical significance was determined using a Friedman test; * - $P < 0.05$; ** - $P < 0.01$. F) Quantification of the amplitude of the tail currents induced by 1 μM of *cis*-Azoveratridine at different membrane potentials (-50, 0 and +30 mV). Light gray bars represent the current amplitude in controls; dark grey bars represent the amplitude after addition of non-illuminated *trans*-enriched Azoveratridine; violet bars show the responses to 365 nm light (*cis*-enriched Azoveratridine); and orange bars indicate the effect of TTX application. Data are represented by mean ± SEM. Statistical significance of the difference between groups was determined using a Friedman test; n = 10 cells, ** - $P < 0.01$; **** - $P < 0.0001$. G) Non-linear fits of the tail current decay in control (light gray line), after application of Azoveratridine (dark gray line) and upon simultaneous application of Azoveratridine and 365 nm light (violet line, *cis*-enriched Azoveratridine). H) Recovery (decay) time of the tail current (τ, s) induced by application of 3 μM Azoveratridine at 0 and + 30 mV. The bar colors are as in panel G, the data are represented by mean ± SEM, and the statistical analysis was done using a Friedman test; n = 6 cells; ns - not significant; * - $P < 0.05$.

wave along the axon. About 1 ms after the opening, Na_V channels start to inactivate (transit to the closed state), contributing to the recovery of the neuron's resting potential (together with the opening of voltage-gated K^+ channels). Veratridine disrupts the inactivation process and effectively prolongs the channel's open state and neuronal depolarization by presumably binding to the pore of Na_V channels. This interference with inactivation ultimately inhibits the proper propagation of action potentials [30,41]. In cardiac myocytes, Na_V channels coordinate heart contraction by depolarizing the cell membrane and propagating cardiac action potentials [42,43]. Veratridine enhances myocardial contractility by indirectly increasing cytoplasmatic levels of Ca^{2+}, prolonging action potential, and delaying repolarization of heart muscle cells [44,45].

We first studied the effect of Azoveratridine in cultured rat hippocampal neurons using patch clamp electrophysiology. The protocol to record Na_V-mediated currents is shown in Fig. 3.A: neurons were held at –70 mV, a prepulse to –120 mV was applied to relieve Na_V channel inactivation and then 10 mV incremental voltage steps of 200 ms were applied from –70 mV to + 30 mV [46]. Upon application of 1 μM Azoveratridine at the benchtop condition without illumination (*trans*-enriched, see Fig. 2.C), a tail current was observed during repolarization (Fig. 3.B, black trace). When the cell was subsequently illuminated with 365 nm light (*cis*-enriched Azoveratridine), the amplitude of the tail current increased (Fig. 3.B, violet trace). This current was blocked by the application of tetrodotoxin (TTX), a potent inhibitor of Na_V channels (Fig. 3.B, orange trace), as reported for veratridine [47].

Azoveratridine increased the tail current amplitude in a concentration-, voltage-, and isomer-dependent manner (Fig. 3.CDE). The amplitude of the tail current induced by UV light at + 30 mV increased with the concentration (Fig. 3.CDE): at 0.6 μM it changed from −126 ± 27 pA to −200 ± 32 pA (n = 4, P < 0.05 with Friedman test), at 1 μM from −71 ± 17 pA to −324 ± 69 pA (n = 10, P < 0.01 with Friedman test) and at 3 μM from −94 ± 34 pA to −435 ± 80 pA (n = 6, P < 0.01 with Friedman test). The effect of illuminating Azoveratridine was more pronounced at positive potentials (Fig. 3.CDE). To study the voltage dependence of the tail current, we compared the effects of 1 μM Azoveratridine at −50, 0, and + 30 mV. At −50 mV we did not observe a tail current after addition of Azoveratridine, either before or after illumination (Fig. 3.CDEF), whereas 0 and + 30 mV steps yield a statistically significant current increase compared to the control, respectively, from −58 ± 21 pA to −271 ± 53 pA and from −71 ± 17 pA to −342 ± 69 pA (P < 0.01, Friedman test). Tail currents display a single exponential decay (Fig. 3.G). Upon addition of 3 μM Azoveratridine at 0 mV in the dark, the lifetime (τ) increased from 0.12 ± 0.03 s to 0.92 ± 0.3 s and at + 30 mV from 0.16 ± 0.03 s to 0.61 ± 0.14 s (n = 6) but these changes were not statistically significant (P > 0.05, Friedman test). However, 365 nm light increased τ significantly to 1.16 ± 0.2 s at 0 mV and to 1.44 ± 0.4 s at + 30 mV (P < 0.05 according to Friedman test; Fig. 3.H).

Thus, Azoveratridine induces tail currents in neurons, modulates their amplitude and time course in a light- and dose-dependent manner, and this effect is abolished by TTX, demonstrating that they are mediated by Na_V channels. The pharmacological profile of Azoveratridine in

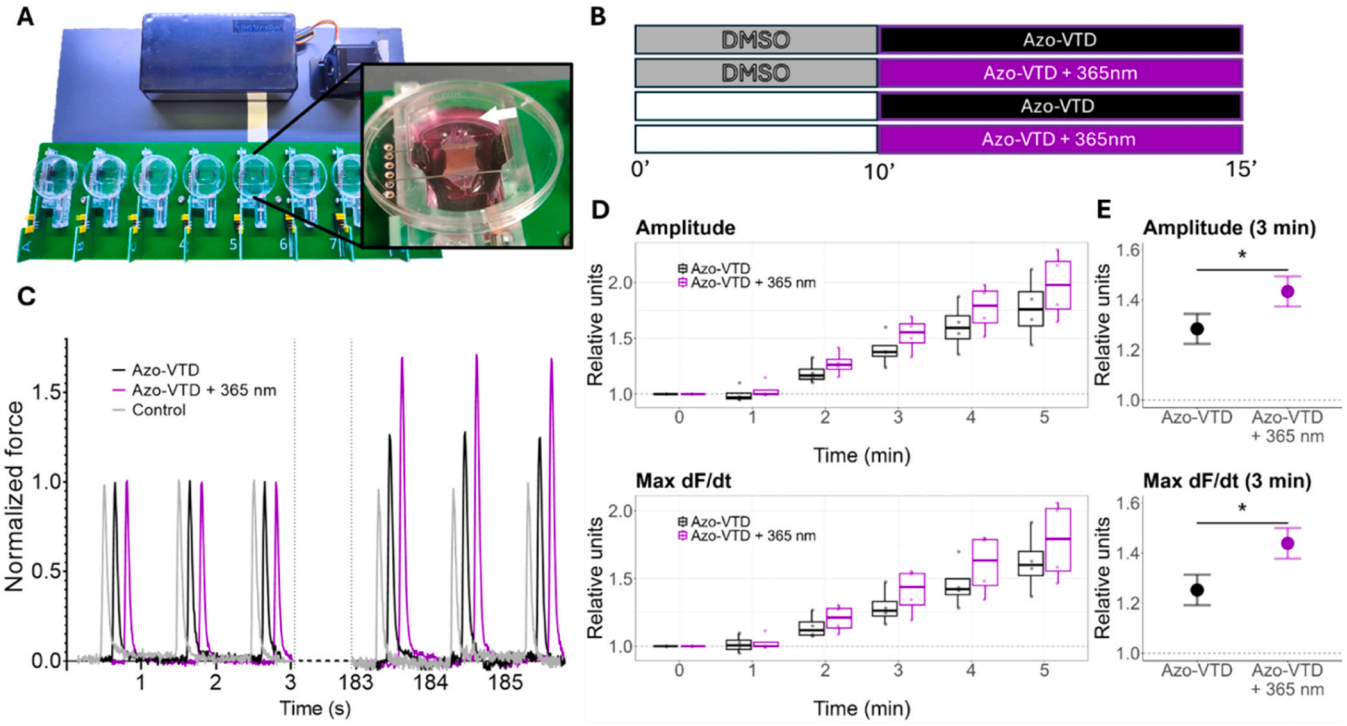

Fig. 4. Effect of Azoveratridine (Azo-VTD) in myocardial slices. A) Experimental setup. Picture of the eight-channel biomimetic cultivation chambers which allow simultaneous recording of up to 8 living myocardial slices (LMS) with different biochemical and stimulation conditions. The figure inset shows an LMS (arrow) placed in the working system. B) Schematic summary of the experimental design. In two channels, DMSO (vehicle) was initially added to the LMS as a control, and 3 μM non-illuminated Azoveratridine or pre-illuminated Azoveratridine were subsequently added. The Azoveratridine solvent (DMSO) did not affect contractility parameters. In five additional channels per group, non-illuminated Azoveratridine or pre-illuminated Azoveratridine were applied without previous addition of DMSO. C) Representative recordings of three LMS under the three experimental conditions (control with DMSO only, 3 μM non-illuminated Azoveratridine, and 3 μM 365 nm pre-illuminated Azoveratridine). The first three peaks are LMS contraction responses at baseline; the last three peaks are contraction responses 3 min after adding DMSO, non-illuminated Azoveratridine or pre-illuminated Azoveratridine. Values are normalized to the maximum amplitude at baseline, and groups nudged 200 ms to enable curve visualization. D) Quantification (boxplot) of normalized force amplitude (upper panel) and maximum force development rate dF/dt (lower panel) measurement in the non-illuminated and pre-illuminated Azoveratridine groups at baseline and in the first 5 min after adding the experimental compound (n = 4 slices per group). E) Amplitude (upper panel) and maximum dF/dt (lower panel) 3 min after adding the experimental compound in the two groups (n = 6 slices per group). The estimated marginal means and SEM are plotted. Analyses conducted with a linear mixed effects model including experimental group as a fixed factor and every batch as a random effect; the group factor was significant at the P < 0.05 level (*).

different channel subtypes and whether it is altered with respect to that of veratridine will be evaluated in future studies.

Since Na_V channels are also extensively expressed in the heart, we tested Azoveratridine using a living myocardial slices (LMS) assay. We compared the effects of non-illuminated (benchtop condition) and 365 nm pre-illuminated Azoveratridine *ex vivo* in an LMS setup of ventricular myocardium, in which Na_V channels are central to contractility. Our instrument allows measuring the mechanical contraction force elicited by electric pulses applied simultaneously and independently to eight rat myocardial slices (Fig. 4.A). The time course of the experiment is shown in Fig. 4.B. Representative recordings of the contraction force of myocardial slices in control condition and in both experimental groups are shown in Fig. 4.C. The force amplitude and maximum force development rate (dF/dt) differed between groups few minutes after adding 3 μM Azoveratridine in the dark and 3 μM UV pre-illuminated Azoveratridine (Fig. 4.D). We compared both parameters at minute 3 after incubation and found that pre-illuminated Azoveratridine induced a significantly higher increase in amplitude and maximum dF/dt compared with non-illuminated Azoveratridine. These results demonstrate that Azoveratridine acutely heightens the contractility of cardiac tissue and that its *cis* isoform is more active than its *trans*-isoform (Fig. 4.E).

Natural products have been the cornerstone of medicine to treat a wide variety of diseases. Their structures also provided cues to discover new drugs. Notable examples include paclitaxel (anticancer drug), morphine and salicylic acid (analgesic drugs), artemisinin (antimalarial), vancomycin (antibacterial), coumarins (anticoagulant) and digoxin (cardiovascular) [48–52]. In this work, we focused on a specific class of natural products: toxins. While traditionally classified as hazardous substances, we aimed to develop a method to regulate their biological activity for transforming them into valuable pharmacological tools. We have shown that their activity can be adjusted using light by inserting a photoswitch in the structure, to reduce undesired effects while exploiting their effectiveness and target selectivity. This approach in combination with focalized illumination may allow to repurpose toxins and increase their safety index. Importantly, the photoswitch can be introduced chemically by late-stage modifications of the native toxin scaffold.

In this context, late-stage modifications of natural products provide an efficient strategy to generate derivatives for drug discovery and chemical biology [53]. In fact, traditional total synthesis of natural compounds is often challenging and laborious with long synthetic pathways that can be time-consuming and inefficient. Therefore, direct modifications of natural compounds have gained interest to create new derivatives and explore their structure–activity and structure–property relationships while avoiding the difficulty of total synthesis [54–56].

However, the complexity of natural products bearing diverse and reactive functional groups is often a barrier for selective late-stage functionalization [53,57,58]. Recently, significant progress has been made in organic chemistry with the development of site-selective synthetic methodologies including C-H functionalization [59–61], bio catalysis [57,58,62], synthetic catalysis [56,63], photochemistry [64–66], and electrochemistry [67,68].

Here we explored different methods for late-stage C-H nitration of veratridine, which is a key step for further derivatization. Nitro groups are highly versatile functional groups that can serve as intermediate to amines, cross-coupling reactions, or heterocycles [69,70]. However, conventional nitration protocols involve harsh conditions using nitric acid and sulfuric acid which can be particularly damaging to the delicate and complex structure of natural products such as toxins. In our case, even the nitration of veratridine by transition-metal catalysts in the presence of stoichiometric amounts of nitric acid [71,72] led to degradation of the toxin.

To overcome the downsides of using strong acids, recent efforts have focused on developing alternative methods to prepare nitroarenes under milder conditions [71,73–75]. For example, metal nitrates (such as Al $(NO_3)_3$ and $Fe(NO_3)_3{\cdot}9\ H_2O$) offer a valuable alternative nitro source as safe, easy to handle, and inexpensive reagents [61,76,77]. Here for the first time we successfully achieved the nitration of veratridine by using a common salt such as KNO_3 in the presence of aluminium trichloride and trimethylchlorosilane [78]. The difficulties to consistently reproduce the reaction conditions encouraged us to use another inorganic salt such as nitronium tetrafluoroborate (BNO_2F_4) [79,80]. Nitration of veratridine by BNO_2F_4 proceeded relatively fast, cleanly, and in good yields, offering an extremely simple, low-cost and highly effective alternative for nitration in mild conditions. This nitration method is useful beyond its success with veratridine, because it does not require the use of acids to generate the nitronium ion and it suits acid-sensitive substrates. Its anhydrous conditions benefit moisture-sensitive compounds, and the low reaction temperatures (0 °C to room temperature) make it compatible with thermally sensitive materials. These features make BNO_2F_4-mediated nitration a promising option for structurally delicate or functionally complex molecules.

In summary, while diazonium salts failed to afford one-step derivatization of veratridine, we investigated three different methods for late-stage C-H nitration and successfully validated two of them. Overall, the salt BNO_2F_4 gave more reproducible results and offered milder conditions as nitrating reagent, hence it was considered preferable. The introduction of the nitro group in the veratroyl moiety of the toxin allowed its final derivatization with azobenzene. Remarkably, this modification is compatible with the activity of the toxin [28,30,32,33] and allows to inhibit it in the dark (*trans* isomer) and restore it upon 365 nm light illumination (*cis* isomer). Although the switching process requires UV light, it is feasible to incorporate substituted azobenzenes or different photoswitches to red-shift the absorption spectrum in future studies [81–84]. Alternatively, multiphoton excitation allows photoswitching with tissue-penetrating infrared light [85].

The photoconversion of Azoveratridine is moderately effective but not quantitative, resulting in *trans*- or *cis*-enriched solutions after irradiation. Nevertheless, this level of conversion is sufficient to significantly change the activity of Azoveratridine with illumination in neurons and cardiac tissue. This indicates that the two isomers have different potency (*cis* being more active than *trans*) and that a low concentration of the *cis* isomer is enough to trigger a pharmacological response. To improve these properties, quantitative photoconversion might be achieved with alternative switches such as azoheteroaryls, that are compatible with this approach [86,87].

The late-stage modification of veratridine reported here (Scheme 2) lays the ground for other derivatizations including photoswitches responsive to visible light, and radioactive, fluorescent, or affinity probes to label Na_V channels in tissue. Additionally, other types of late-stage functionalization could be explored to introduce functional groups beyond nitro, further expanding the opportunities to leverage the chemistry and reactivity of veratridine as a versatile pharmacological tool.

In the context of photopharmacology, Azoveratridine is the first photoswitchable alkaloid toxin reported whereas photoswitchable gramicidin and charybdotoxin are peptide-based [25,88]. Moreover, unlike caged saxitoxin derivatives and caged peptide toxins, which require washout to counteract their effect due to the irreversibility of the uncaging process [11,89], Azoveratridine can be switched back and forth between its *trans* and *cis* conformations using different wavelengths of light (Fig. 2). The two isomers exert different biological effects *in vitro,* with *cis*-Azoveratridine displaying higher activity than *trans* in two independent proof-of-concept demonstrations in neurons and cardiac slices. Future work will test the reversibility of Azoveratridine action *in vitro* and *in vivo* to increase its biological relevance.

Azoveratridine is also the first photoswitchable opener of vertebrate sodium channels [90,91] and complements the recently reported photoswitchable blockers [34]. The mechanism by which it increases Na^+ ion flow is probably similar to that of veratridine, namely inducing a hyperpolarizing shift in Na_V channel activation and blocking slow

inactivation, thereby yielding a persistent sodium current [28,92,93]. These effects may be light-dependent due to differences in the shape, volume, and/or polarity of the *trans* and *cis* azobenzene unit on the veratroyl moiety, a structural element known to be critical for toxin activity [28,30,32,33]. Such changes might regulate the binding affinity and/or efficacy of Azoveratridine photoisomers. Investigating the binding and photoswitching mechanisms of Azoveratridine with computational methods will allow to engineer analogs with enhanced properties.

Diverse applications can be envisioned based on the experiments of Figs. 3 and 4. For example, fast temporal photocontrol of Na_V channel inactivation could be useful to investigate toxin binding dynamics and its voltage-gated ion channel gating [94]. Na_V channels could also be functionally mapped in cells using fluorescent voltage sensors and focalized photostimulation, potentially at subcellular resolution. At a larger scale, projecting spatiotemporal light patterns on nervous and cardiac tissue in the presence of Azoveratridine could provide insights into brain circuits and functional regions of the heart. For example, spatially and temporally selective photoactivation of Na_V channels might resolve the uncertainties regarding the differential contribution of cardiac regions and targets to arrhythmogenicity [95], such as the right ventricular outflow tract in Brugada syndrome or different myocardial layers from epicardium to midmyocardium to endocardium [96,97]. Modulating Na_V channel function could also be used to acutely increase contractility, and may provide high physiological relevance in human cardiomyocytes and cardiac slices, and in animal models.

Azoveratridine may also be useful to study the role of VGSC that are overexpressed in certain cancers, although the exploration of pharmacotherapies in these cases involves mostly channel inhibitors [98–101]. Notably, azologs of quercetin would be straightforward to obtain to evaluate the benefits of localized photoinhibition of tumor growth.

Veratridine was tested in human muscles as a treatment against myasthenia gravis, a neuromuscular junction disease that causes severe muscular weakness [102,103]. The toxin effectively increased muscular tonus and helped muscles to contract, but systemic toxicity was a concern for further applications. Given the effects of sodium blockade in the vessels, *veratrum* alkaloids were also clinically tested to treat hypertension, but their therapeutic window (i.e., the dose difference between efficacy and adverse effects) were extremely narrow [104]. In addition to its established neurotoxicity, veratridine may cause unpredictable bradycardia and hypotension by stimulating afferent vagal nerve endings in the heart and by affecting peripheral vascular resistance [105,106] in an heterogeneous manner in different vascular beds [107,108]. Altogether, these resulted in uncontrolled and dangerous drops in blood pressure, rendering veratridine clinically ineffective [106]. All these limitations with systemically administered toxins are linked to the impossibility to target them to specific locations (e.g., at a selected artery without affecting other areas). The potential use of systemically administered sodium channel blockers to treat cardiac arrhythmia and cancer faces similar challenges [95,98]. A dark-inactive, light-activated toxin like Azoveratridine may help to overcome these hurdles, enabling precise, on demand sodium channel modulation while reducing the risk of systemic adverse effects.

3. Conclusions

To address the need of potent and selective pharmacological tools, we have introduced two methods for late-stage C-H nitration and subsequent derivatization of the natural toxin veratridine and developed a photoswitchable analogue with an azobenzene moiety attached to the veratroyl group (Azoveratridine). We have characterized its chemical, photochemical, and biological properties, and demonstrated that Azoveratridine displays aqueous solubility, reversible photoisomerization, and light-dependent activity in neurons and myocardial slices. Azoveratridine is the first photoswitchable alkaloid toxin and vertebrate sodium channel opener. These results demonstrate the feasibility of harnessing toxin activity with light for fundamental pharmacological research and to open the way to clinical applications requiring focalized, on demand, and reversible drug activity.

CRediT authorship contribution statement

Luisa Camerin: Writing – review & editing, Writing – original draft, Methodology, Investigation, Formal analysis, Data curation. **Galyna Maleeva:** Writing – review & editing, Writing – original draft, Methodology, Investigation, Formal analysis, Data curation. **Ailín Ramírez-Abreu:** Writing – review & editing, Methodology, Investigation, Formal analysis, Data curation. **Víctor Cilleros-Mañé:** Writing – review & editing, Methodology, Formal analysis, Data curation. **Drilon Miftari:** Writing – review & editing, Methodology, Investigation, Formal analysis, Data curation. **Montserrat Batlle:** Writing – review & editing, Methodology, Investigation, Formal analysis, Data curation. **Carlo Matera:** Writing – review & editing, Supervision, Methodology. **Eduard Guasch:** Writing – review & editing, Supervision, Project administration, Methodology, Funding acquisition, Formal analysis, Data curation. **Pau Gorostiza:** Writing – review & editing, Writing – original draft, Supervision, Resources, Project administration, Funding acquisition, Conceptualization.

Declaration of Competing Interest

The authors declare that they have no known competing financial interests or personal relationships that could have appeared to influence the work reported in this paper.

Acknowledgements

The authors wish to thank Ramon Eritja, Ramona Santini, and Samuel Ojosnegros for useful discussions. This research was funded by the EU Horizon 2020 and Horizon Europe Framework Programmes for Research and Innovation, including the European Innovation Council Pathfinder Open (Phototheraport, 101130883), Human Brain Project (WaveScalES, SGA3, 945539), and Information and Communication Technologies (Deeper, ICT-36–2020–101016787). It was also supported by the Government of Catalonia (CERCA Programme; AGAUR 2021-SGR-01410); by the Spanish Ministry of Science and Innovation (DEEP RED, grant PID2019–111493RB-I00; EPILLUM, grant PID2022–142609OB-I00 funded by AEI/10.13039/501100011033/ FEDER, UE; Research Network in Biomedicine eBrains-Spain, RED2022–134823-E); and by the Instituto de Salud Carlos III (FIS grant PI22/00953) L. C. was supported by a fellowship from AGAUR (FI-2020, 2020 FI-B-00660). G. M. was supported by a Ramón y Cajal Investigator grant (RYC2021–033056-I financed by MCIN/AEI /10.13039/501100011033 and by European Union NextGeneration EU/PRTR). A. R.-A. was supported by a Ph. D. fellowship from AEI (PREP2022–000244 associated to grant PID2022–142609OB-I00). V. C.-M. was supported by a Juan de la Cierva fellowship (JDC2022–049863-I) financed by MCIU/AEI/10.13039/ 501100011033.

All experiments on animals were conducted in compliance with EU directive 2010/63/EU and Spanish guidelines (Laws 32/2007, 6/2013, and RD 53/2013) and were authorized by the Parc Científic de Barcelona and Universitat de Barcelona Animal Research Ethics Committees and by the Government of Catalonia (codes 21–000-PG and 11273).

Appendix A. Supporting information

Supplementary data associated with this article can be found in the online version at doi:10.1016/j.biopha.2026.119546.

Data availability

Data will be made available on request.

References

[1] D. Sun, W. Gao, H. Hu, S. Zhou, Why 90% of clinical drug development fails and how to improve it? Acta Pharm. Sin. B 12 (2022) 3049–3062.
[2] W.A. Catterall, S. Cestèle, V. Yarov-Yarovoy, H.Y. Frank, K. Konoki, T. Scheuer, Voltage-gated ion channels and gating modifier toxins, Toxicon 49 (2007) 124–141.
[3] D.L.J. Quicke, M. Ghafouri Moghaddam, B.A. Butcher, Dietary challenges for parasitoid wasps (Hymenoptera: Ichneumonoidea); coping with toxic hosts, or not? Toxins 15 (2023) 424.
[4] K. Kshatriya, J. Gershenzon, Disarming the defenses: insect detoxification of plant defense-related specialized metabolites, Curr. Opin. Plant Biol. 81 (2024) 102577.
[5] H.B. Fiorotti, S.G. Figueiredo, F.V. Campos, D.C. Pimenta, Cone snail species off the Brazilian coast and their venoms: a review and update, J. Venom. Anim. Toxins Incl. Trop. Dis. 29 (2023) e20220052.
[6] G.H. Beale, A. Jurand, J.R. Preer, The classes of endosymbiont of Paramecium aurelia, J. Cell Sci. 5 (1969) 65–91.
[7] S. Singh, A. Singh, V. Baweja, A. Roy, A. Chakraborty, I.K. Singh, Molecular rationale of insect-microbes symbiosis—from insect behaviour to Mechanism, Microorganisms 9 (2021) 2422.
[8] V. Ruta, Y. Jiang, A. Lee, J. Chen, R. MacKinnon, Functional analysis of an archaebacterial voltage-dependent K+ channel, Nature 422 (2003) 180–185.
[9] S.L. Gopalakrishnakone, P. Lourdes, J. Cruz, Toxins and Drug Discovery, Springer Nature, 2017.
[10] N. Ohyabu, T. Nishikawa, M. Isobe, First asymmetric total synthesis of tetrodotoxin, J. Am. Chem. Soc. 125 (2003) 8798–8805.
[11] H. Tanino, T. Nakata, T. Kaneko, Y. Kishi, A stereospecific total synthesis of dl-saxitoxin, J. Am. Chem. Soc. 99 (1977) 2818–2819.
[12] K.C. Nicolaou, Organic synthesis: the art and science of replicating the molecules of living nature and creating others like them in the laboratory, Proc. R. Soc. A Math. Phys. Eng. Sci. 470 (2014) 20130690.
[13] D.B. Konrad, K.-P. Rühmann, H. Ando, B.E. Hetzler, N. Strassner, K.N. Houk, B. S. Matsuura, D. Trauner, A concise synthesis of tetrodotoxin, Science (1979) 377 (2022) 411–415.
[14] S. Wiere, C. Sugai, M.J. Espiritu, V.P. Aurelio, C.D. Reyes, N. Yuzon, R.M. Whittal, J. Tytgat, S. Peigneur, J.-P. Bingham, Research into the Bioengineering of a Novel α-Conotoxin from the Milked Venom of Conus obscurus, Int. J. Mol. Sci. 23 (2022) 12096.
[15] H.S. Mosher, F.A. Fuhrman, H.D. Buchwald, H.G. Fischer, Tarichatoxin—Tetrodotoxin: A Potent Neurotoxin: A nonprotein substance isolated from the California newt is the same as the toxin from the puffer fish, Science (1979) 144 (1964) 1100–1110.
[16] A. Yokoyama, M. Murata, Y. Oshima, T. Iwashita, T. Yasumoto, Some chemical properties of maitotoxin, a putative calcium channel agonist isolated from a marinedinoflagellate, J. Biochem. 104 (1988) 184–187.
[17] B.Z. Horowitz, Botulinum toxin, Crit. Care Clin. 21 (2005) 825–839.
[18] A.L. Oliveira, M.F. Viegas, S.L. da Silva, A.M. Soares, M.J. Ramos, P.A. Fernandes, The chemistry of snake venom and its medicinal potential, Nat. Rev. Chem. 6 (2022) 451–469.
[19] K. de, C.F. Bordon, C.T. Cologna, E.C. Fornari-Baldo, E.L. Pinheiro-Júnior, F. A. Cerni, F.G. Amorim, F.A.P. Anjolette, F.A. Cordeiro, G.A. Wiezel, I.A. Cardoso, From animal poisons and venoms to medicines: achievements, challenges and perspectives in drug discovery, Front. Pharm. 11 (2020) 1132.
[20] J.P. Robinson, J.B. Picklesimer, D. Puett, Tetanus toxin. The effect of chemical modifications on toxicity, immunogenicity, and conformation, J. Biol. Chem. 250 (1975) 7435–7442.
[21] K. Sandvig, S. Olsnes, A. Pihl, Chemical modifications of the toxic lectins abrin and ricin, Eur. J. Biochem 84 (1978) 323–331.
[22] A. Habeeb, Some studies on the chemical modification of ϵ-toxin of Clostridium perfringens type D, Biochim. Biophys. Acta 74 (1963) 113–121.
[23] C. Pederzolli, L. Cescatti, G. Menestrina, Chemical modification ofStaphylococcus aureus α-toxin by diethylpyrocarbonate: Role of histidines in its membrane-damaging properties, J. Membr. Biol. 119 (1991) 41–52.
[24] B. Walker, H. Bayley, Key Residues for Membrane Binding, Oligomerization, and Pore Forming Activity of Staphylococcal α-Hemolysin Identified by Cysteine Scanning Mutagenesis and Targeted Chemical Modification (*), J. Biol. Chem. 270 (1995) 23065–23071.
[25] T. Lougheed, V. Borisenko, T. Hennig, K. Rück-Braun, G.A. Woolley, Photomodulation of ionic current through hemithioindigo-modified gramicidin channels, Org. Biomol. Chem. 2 (2004) 2798–2801.
[26] M. Ohta, T. Narahashi, R.F. Keeler, Effects of veratrum alkaloids on membrane potential and conductance of squid and crayfish giant axons, J. Pharmacol. Exp. Ther. 184 (1973) 143–154.
[27] A. Niitsu, A. Egawa, K. Ikeda, K. Tachibana, T. Fujiwara, Veratridine binding to a transmembrane helix of sodium channel Nav1. 4 determined by solid-state NMR, Bioorg. Med. Chem. 26 (2018) 5644–5653.
[28] J.D.B. Robert, A. Craig II, Catherine E. Garrison, Phuong T. Nguyen, Vladimir Yarov-Yarovoy, Veratridine a janus-faced modulator of voltage gated sodium ion channels.pdf, ACS Chem. Neurosci. (2020).
[29] D.B. Tikhonov, B.S. Zhorov, Sodium channel activators: model of binding inside the pore and a possible mechanism of action, FEBS Lett. 579 (2005) 4207–4212.
[30] A. Gulsevin, A.M. Glazer, T. Shields, B.M. Kroncke, D.M. Roden, J. Meiler, Veratridine Can Bind to a Site at the Mouth of the Channel Pore at Human Cardiac Sodium Channel NaV1. 5, Int. J. Mol. Sci. 2225 (2022) *23*.
[31] M. Volgraf, P. Gorostiza, S. Szobota, M.R. Helix, E.Y. Isacoff, D. Trauner, Reversibly caged glutamate: a photochromic agonist of ionotropic glutamate receptors, J. Am. Chem. Soc. 129 (2007) 260–261.
[32] A. Niitsu, M. Harada, T. Yamagaki, K. Tachibana, Conformations of 3-carboxylic esters essential for neurotoxicity in veratrum alkaloids are loosely restricted and fluctuate, Bioorg. Med. Chem. 16 (2008) 3025–3031.
[33] I. Ujvary, B.K. Eya, R.L. Grendell, R.F. Toia, J.E. Casida, Insecticidal activity of various 3-acyl and other derivatives of veracevine relative to the Veratrum alkaloids veratridine and cevadine, J. Agric. Food Chem. 39 (1991) 1875–1881.
[34] L. Camerin, G. Maleeva, A.M.J. Gomila, I. Suárez-Pereira, C. Matera, D. Prischich, E. Opar, F. Riefolo, E. Berrocoso, P. Gorostiza, Photoswitchable Carbamazepine Analogs for Non-Invasive Neuroinhibition In Vivo, Angew. Chem. (2024) e202403636.
[35] D. Prischich, A.M.J. Gomila, S. Milla-Navarro, G. Sangüesa, R. Diez-Alarcia, B. Preda, C. Matera, M. Batlle, L. Ramírez, E. Giralt, Adren. Modul. Photo Ligands Angew. Chem. Int. Ed. 60 (2021) 3625–3631.
[36] Z. Ahmed, A. Siiskonen, M. Virkki, A. Priimagi, Controlling azobenzene photoswitching through combined ortho-fluorination and-amination, Chem. Commun. 53 (2017) 12520–12523.
[37] M. Dong, A. Babalhavaeji, S. Samanta, A.A. Beharry, G.A. Woolley, Red-shifting azobenzene photoswitches for in vivo use, Acc. Chem. Res. 48 (2015) 2662–2670.
[38] C. Knie, M. Utecht, F. Zhao, H. Kulla, S. Kovalenko, A.M. Brouwer, P. Saalfrank, S. Hecht, D. Bléger, Ortho-Fluoroazobenzenes: Visible Light Switches with Very Long-Lived Z Isomers *Chemistry*, A Eur. J. 20 (2014) 16492–16501.
[39] S. Samanta, T.M. McCormick, S.K. Schmidt, D.S. Seferos, G.A. Woolley, Robust visible light photoswitching with ortho-thiol substituted azobenzenes, Chem. Commun. 49 (2013) 10314–10316.
[40] D.M. Brill, J.A. Wasserstrom, Intracellular sodium and the positive inotropic effect of veratridine and cardiac glycoside in sheep Purkinje fibers, Circ. Res. 58 (1986) 109–119.
[41] H.L. Zhu, R.D. Wassall, M. Takai, H. Morinaga, M. Nomura, T.C. Cunnane, N. Teramoto, Actions of veratridine on tetrodotoxin-sensitive voltage-gated Na+ currents, NaV1.6, in murine vas deferens myocytes, Br. J. Pharm. 157 (2009) 1483–1493.
[42] X.-G. Zong, M. Dugas, P. Honerjäger, Relation between veratridine reaction dynamics and macroscopic Na current in single cardiac cells, J. Gen. Physiol. 99 (1992) 683–697.
[43] P. Honerjäger, M. Reiter, The relation between the effects of veratridine on action potential and contraction in mammalian ventricular myocardium, Naunyn. Schmiede Arch. Pharm. 289 (1975) 1–28.
[44] T. Henden, T.S. Larsen, D.A. Lathrop, Effect of stimulation and veratrine on total cellular calcium in rat and guinea-pig ventricular myocytes, Basic Res. Cardiol. 88 (1993) 557–565.
[45] D. Wermelskirchen, B. Wilffert, U. Nebel, A. Wirth, T. Peters, Veratridine-induced intoxication in the isolated left atrium of the rat: effects of some anti-ischemic compounds *Naunyn*, Schmiede Arch. Pharm. 344 (1991) 101–106.
[46] H. Zhu, R.D. Wassall, M. Takai, H. Morinaga, M. Nomura, T.C. Cunnane, N. Teramoto, Actions of veratridine on tetrodotoxin-sensitive voltage-gated Na+ currents, NaV1. 6, in murine vas deferens myocytes, Br. J. Pharm. 157 (2009) 1483–1493.
[47] K.A. Alkadhi, L.-M. Tian, Veratridine-enhanced persistent sodium current induces bursting in CA1 pyramidal neurons, Neuroscience 71 (1996) 625–632.
[48] D.A. Dias, S. Urban, U. Roessner, A historical overview of natural products in drug discovery, Metabolites 2 (2012) 303–336.
[49] A.G. Atanasov, S.B. Zotchev, V.M. Dirsch, C.T. Supuran, Natural products in drug discovery: advances and opportunities, Nat. Rev. Drug Discov. 20 (2021) 200–216.
[50] D.J. Newman, G.M. Cragg, Natural products as sources of new drugs over the 30 years from 1981 to 2010, J. Nat. Prod. 75 (2012) 311–335.
[51] J. Sharifi-Rad, N. Cruz-Martins, P. López-Jornet, E.P.-F. Lopez, N. Harun, B. Yeskaliyeva, A. Beyatli, O. Sytar, S. Shaheen, F. Sharopov, Natural coumarins: exploring the pharmacological complexity and underlying molecular mechanisms, Oxid. Med. Cell. Longev. 2021 (2021) 6492346.
[52] M. Gheorghiade, K.F. Adams, Jr, W.S. Colucci, Digoxin in the management of cardiovascular disorders, Circulation 109 (2004) 2959–2964.
[53] B. Hong, T. Luo, X. Lei, Late-stage diversification of natural products, ACS Cent. Sci. 6 (2020) 622–635.
[54] K.C. Morrison, P.J. Hergenrother, Natural products as starting points for the synthesis of complex and diverse compounds, Nat. Prod. Rep. 31 (2014) 6–14.
[55] P. Waelès, M. Gauthier, F. Coutrot, Challenges and Opportunities in the Post-Synthetic Modification of Interlocked, Mol. Angew. Chem. Int. Ed. 60 (2021) 16778–16799.
[56] C.R. Shugrue, S.J. Miller, Applications of nonenzymatic catalysts to the alteration of natural products, Chem. Rev. 117 (2017) 11894–11951.
[57] N.D. Fessner, P450 monooxygenases enable rapid late-stage diversification of natural products via C− H bond activation, ChemCatChem 11 (2019) 2226–2242.
[58] S.J. Benkovic, S. Hammes-Schiffer, A perspective on enzyme catalysis, Science (1979) 301 (2003) 1196–1202.
[59] K. Godula, D. Sames, CH bond functionalization in complex organic synthesis, Science (1979) 312 (2006) 67–72.

[60] J.F. Hartwig, Evolution of C–H bond functionalization from methane to methodology, J. Am. Chem. Soc. 138 (2016) 2–24.
[61] Y. Zheng, Q.-Q. Hu, Q. Huang, Y. Xie, Late-Stage C–H Nitration of Unactivated Arenes by Fe (NO3) 3· 9H2O in Hexafluoroisopropanol, Org. Lett. 26 (2024) 3316–3320.
[62] J.C. Lewis, P.S. Coelho, F.H. Arnold, Enzymatic functionalization of carbon–hydrogen bonds, Chem. Soc. Rev. 40 (2011) 2003–2021.
[63] R.R. Karimov, J.F. Hartwig, Transition-metal-catalyzed selective functionalization of C (sp3)− H bonds in natural products, Angew. Chem. Int. Ed. 57 (2018) 4234–4241.
[64] C.K. Prier, D.A. Rankic, D.W.C. MacMillan, Visible light photoredox catalysis with transition metal complexes: applications in organic synthesis, Chem. Rev. 113 (2013) 5322–5363.
[65] K.L. Skubi, T.R. Blum, T.P. Yoon, Dual catalysis strategies in photochemical synthesis, Chem. Rev. 116 (2016) 10035–10074.
[66] T. Long, L. Liu, Y. Tao, W. Zhang, J. Quan, J. Zheng, J.D. Hegemann, M. Uesugi, W. Yao, H. Tian, Light-controlled tyrosine nitration of proteins, Angew. Chem. Int. Ed. 60 (2021) 13414–13422.
[67] J. Yoshida, K. Kataoka, R. Horcajada, A. Nagaki, Modern strategies in electroorganic synthesis, Chem. Rev. 108 (2008) 2265–2299.
[68] E.J. Horn, B.R. Rosen, P.S. Baran, Synthetic organic electrochemistry: an enabling and innately sustainable method, ACS Cent. Sci. 2 (2016) 302–308.
[69] S. Patra, I. Mosiagin, R. Giri, D. Katayev, Organic nitrating reagents, Synthesis (Stuttg) 54 (2022) 3432–3472.
[70] C. Kannigadu, D.D. N'Da, Recent advances in the synthesis and development of nitroaromatics as anti-infective drugs, Curr. Pharm. Des. 26 (2020) 4658–4674.
[71] Abdulla, S. Amina, Y.A. Kumar, M. Arifuddin, K.C. Rajanna, Mild and efficient nitration of aromatic compounds mediated by transition-metal complexes, Synth. Commun. 41 (2011) 2946–2951.
[72] L. Lu, H. Liu, R. Hua, HNO3/HFIP: a nitrating system for arenes with direct observation of π-complex intermediates, Org. Lett. 20 (2018) 3197–3201.
[73] R. Calvo, K. Zhang, A. Passera, D. Katayev, Facile access to nitroarenes and nitroheteroarenes using N-nitrosaccharin, Nat. Commun. 10 (2019) 3410.
[74] I. Mosiagin, A.J. Fernandes, A. Budinská, L. Hayriyan, K.E.O. Ylijoki, D. Katayev, Catalytic ipso-Nitration of Organosilanes Enabled by Electrophilic N-Nitrosaccharin Reagent, Angew. Chem. 135 (2023) e202310851.
[75] T. Yang, X. Li, S. Deng, X. Qi, H. Cong, H.-G. Cheng, L. Shi, Q. Zhou, L. Zhuang, From N–H Nitration to Controllable Aromatic Mononitration and Dinitration—The Discovery of a Versatile and Powerful N-Nitropyrazole Nitrating Reagent, JACS Au 2 (2022) 2152–2161.
[76] K.A. Juárez-Ornelas, J.O.C. Jiménez-Halla, T. Kato, C.R. Solorio-Alvarado, K. Maruoka, Iodine (III)-catalyzed electrophilic nitration of phenols via non-brønsted acidic NO2+ generation, Org. Lett. 21 (2019) 1315–1319.
[77] Y. He, N. Zhao, L. Qiu, X. Zhang, X. Fan, Regio-and chemoselective mono-and bisnitration of 8-amino quinoline amides with Fe (NO3) 3· 9H2O as promoter and nitro source, Org. Lett. 18 (2016) 6054–6057.
[78] F.F. Van Goor, W.L. Burton, 2011, Google Patents preprint.
[79] G.-F. Huang, P.F. Torrence, Nitration of pyrimidine bases and nucleotides by nitronium tetrafluoroborate. Synthesis of 5-nitro-2'-deoxyuridine, J. Org. Chem. 42 (1977) 3821–3824.
[80] K. Takrouri, T. Chen, E. Papadopoulos, R. Sahoo, E. Kabha, H. Chen, S. Cantel, G. Wagner, J.A. Halperin, B.H. Aktas, Structure–activity relationship study of 4EGI-1, small molecule eIF4E/eIF4G protein–protein interaction inhibitors, Eur. J. Med. Chem. 77 (2014) 361–377.
[81] K. Lützel, H. Laqua, M.B. Sathian, B. Nißl, J.K. Szántó, C.-A. Senser, G. Savasci, L. Allmendinger, B. Kicin, V. Ruf, A Platform for the Development of Highly Red-Shifted Azobenzene-based Optical Tools Angewandte Chemie n.d., e202501779.
[82] A.A. Beharry, O. Sadovski, G.A. Woolley, Azobenzene photoswitching without ultraviolet light, J. Am. Chem. Soc. 133 (2011) 19684–19687.
[83] D. Bléger, J. Schwarz, A.M. Brouwer, S. Hecht, o-Fluoroazobenzenes as readily synthesized photoswitches offering nearly quantitative two-way isomerization with visible light, J. Am. Chem. Soc. 134 (2012) 20597–20600.
[84] S. Samanta, A.A. Beharry, O. Sadovski, T.M. McCormick, A. Babalhavaeji, V. Tropepe, G.A. Woolley, Photoswitching Azo compounds in vivo with red light, J. Am. Chem. Soc. 135 (2013) 9777–9784.
[85] R. Sortino, M. Cunquero, G. Castro-Olvera, R. Gelabert, M. Moreno, F. Riefolo, C. Matera, N. Fernàndez-Castillo, L. Agnetta, M. Decker, Three-Photon Infrared Stimulation of Endogenous Neuroreceptors in Vivo, Angew. Chem. Int. Ed. 62 (2023) e202311181.
[86] J. Calbo, C.E. Weston, A.J.P. White, H.S. Rzepa, J. Contreras-García, M.J. Fuchter, Tuning azoheteroarene photoswitch performance through heteroaryl design, J. Am. Chem. Soc. 139 (2017) 1261–1274.
[87] A. Mukherjee, M.D. Seyfried, B.J. Ravoo, Azoheteroarene and Diazocine Molecular Photoswitches: Self-Assembly, Responsive Materials and Photopharmacology, Angew. Chem. Int. Ed. 62 (2023) e202304437.
[88] Y. Achouba, B. Peres, S. Ascoet, H. Meudal, C. Caumes, C. Zoukimian, H. Millet, M. Choteau-Bodor, C. Carvalhosa, M. Croyal, Photo-isomerization of azobenzene-extended charybdotoxin for the optical control of Kv1. 2 potassium channel activity Angew. Chem. Int. Ed. n.d., e202423278.
[89] A.V. Elleman, G. Devienne, C.D. Makinson, A.L. Haynes, J.R. Huguenard, J. Du Bois, Precise spatiotemporal control of voltage-gated sodium channels by photocaged saxitoxin, Nat. Commun. 12 (2021) 4171.
[90] W. Fu, Y. Ji, Y. Zhang, J. Xu, Z. Xu, J. Cheng, Z. Li, X. Shao, Optical regulation of sodium channels by the azobenzene pyrethrins, ACS Agric. Sci. Technol. 2 (2022) 1311–1317.
[91] Z. Qiao, W. Fu, Y. Zhang, R. Chen, Z. Xu, Z. Li, X. Shao, Azobenzene-semicarbazone enables optical control of insect sodium channels and behavior, J. Agric. Food Chem. 69 (2021) 15554–15561.
[92] W. Ulbricht, The effect of veratridine on excitable membranes of nerve and muscle, Rev. Physiol. Biochem. Exp. Pharmacol. (2010) 18–71.
[93] J.B. Sutro, Kinetics of veratridine action on Na channels of skeletal muscle, J. Gen. Physiol. 87 (1986) 1–24.
[94] W. Ulbricht, Effects of veratridine on sodium currents and fluxes, Rev. Physiol. Biochem. Pharmacol. 133 (2005) 1–54.
[95] Y. Zhou, W. Suo, X. Zhang, J. Lv, Z. Liu, R. Liu, Roles and mechanisms of quercetin on cardiac arrhythmia: a review, Biomed. Pharmacother. 153 (2022) 113447.
[96] C.A. Remme, A.O. Verkerk, W.M.H. Hoogaars, W.T.J. Aanhaanen, B.P. Scicluna, C. Annink, M.J.B. van den Hoff, A.A.M. Wilde, T.A.B. Van Veen, M.W. Veldkamp, The cardiac sodium channel displays differential distribution in the conduction system and transmural heterogeneity in the murine ventricular myocardium, Basic Res. Cardiol. 104 (2009) 511–522.
[97] L. Pannone, D.G. Della Rocca, P. Vergara, A. Sorgente, A. Del Monte, G. Vetta, M. Cespon Fernandez, G. Talevi, I. Eltsov, P.-A. Calburean, In vivo mapping of human ventricular fibrillation in Brugada syndrome: the role of repolarization heterogeneity, Circ. Arrhythm. Electro 17 (2024) e013290.
[98] H. Liu, J. Weng, C.L.-H. Huang, A.P. Jackson, Voltage-gated sodium channels in cancers, Biomark. Res. 12 (2024) 70.
[99] S. Pittolo, X. Gomez-Santacana, K. Eckelt, X. Rovira, J. Dalton, C. Goudet, J.-P. Pin, A. Llobet, J. Giraldo, A. Llebaria, An allosteric modulator to control endogenous G protein-coupled receptors with light, Nat. Chem. Biol. 10 (2014) 813–815.
[100] C. Matera, A.M.J. Gomila, N. Camarero, M. Libergoli, C. Soler, P. Gorostiza, Photoswitchable antimetabolite for targeted photoactivated chemotherapy, J. Am. Chem. Soc. 140 (2018) 15764–15773.
[101] P. Biswas, D. Dey, P.K. Biswas, T.I. Rahaman, S. Saha, A. Parvez, D.A. Khan, N. J. Lily, K. Saha, M. Sohel, A comprehensive analysis and anti-cancer activities of quercetin in ROS-mediated cancer and cancer stem cells, Int. J. Mol. Sci. 23 (2022) 11746.
[102] W.W. Hofmann, Action of veratrine on human skeletal muscle: with special reference to myasthenia gravis, Neurology 8 (1958) 917.
[103] E.G. McGeer, P.L. McGeer, Neurotoxins as tools in neurobiology, Int. Rev. Neurobiol. 22 (1981) 173–204.
[104] L.J. Schep, D.M. Schmierer, J.S. Fountain, Veratrum poisoning, Toxicol. Rev. 25 (2006) 73–78.
[105] J.P. Clozel, T.E. Pisarri, H.M. Coleridge, J.C. Coleridge, Reflex coronary vasodilation evoked by chemical stimulation of cardiac afferent vagal C fibres in dogs, J. Physiol. 428 (1990) 215–232.
[106] E. Meilman, Clinical studies on veratrum alkaloids. III. The effect of protoveratrine on renal function in man, J. Clin. Invest 32 (1953) 80–89.
[107] J. Park, J. Frangieh, L. Réthoré, E. Roy-Vessieres, L. Grimaud, D. Henrion, C. Legendre, C. Legros, Activation of Nav channels by veratridine in mesenteric arteries: contractile or relaxation responses? Arch. Cardiovasc. Dis. Suppl. 13 (2021) 187.
[108] J. Park, C. Sahyoun, J. Frangieh, L. Réthoré, C. Proux, L. Grimaud, E. Vessières, J. Bourreau, C. Mattei, D. Henrion, Veratridine induces vasorelaxation in mouse cecocolic mesenteric arteries, Toxins 16 (2024) 533.